Structure of rapidly quenched glasses in the system Li₂O–SiO₂

N. UMESAKI*
Government Industrial Research Institute, Osaka, 1-8-31, Midorigaoka, Ikeda, Osaka 563, Japan

M. TAKAHASHI
Osaka Municipal Technical Research Institute, Morinomiya, Joto-ku, Osaka 563, Japan

M. TATSUMISAGO, T. MINAMI
Department of Applied Chemistry, University of Osaka Prefecture, Mozu-Umemachi, Sakai, Osaka 591, Japan

Raman spectra of glasses in the Li_2O–SiO_2 system ($41.3 \leqslant Li_2O \leqslant 61.3$ mol%), prepared by rapid quenching, were measured. The proportions of SiO_4 units with 1–4 non-bridging oxygens per silicon (NBO/Si) and the fractions of bridging oxygen, non-bridging oxygen and free or full-active oxygen were determined for these glasses from quantitative analysis of the Raman spectra obtained. X-ray structural analysis of Li_2O–SiO_2 showed an increasing elongation of the average atomic distance of the Si–O pair with increase in Li_2O content due to weakening of the Si–O bond.

1. Introduction

Rapid quenching is one of the useful techniques for developing new glassy materials and for extending the composition range of glass formation. In the system Li_2O–SiO_2, Tatsumisago et al. [1, 2] indicated that rapid quenching extended the limit of glass formation from 40 mol% Li_2O for the usual melt–cooling method up to 66.7 mol % Li_2O, which corresponds to the composition of lithium orthosilicate $2Li_2O \cdot SiO_2$ (Li_4SiO_4); and also indicated that the ratio T_g/T_1 (T_g is the glass transition temperature and T_1 the liquidus temperature) of Li_2O–SiO_2 glass deviated from the so-called "two-thirds rule" ($T_g/T_1 = 2/3$) with increasing Li_2O content. They [3] also found from the density measurement [3] that there is no drastic structural change between rapidly quenched Li_2O–SiO_2 glasses and the corresponding crystals when the Li_2O content is increased. Molecular Dynamics (MD) results [4, 5] for the Li_4SiO_4 melt and glass have revealed that this glass consists of some discrete SiO_4 units with 2–4 non-bridging oxygens per Si (NBO/Si) because of the freezing of the corresponding melt by the rapid quenching. Therefore, these new glasses which result from the extension of the glass-forming region are of great structural interest since a three-dimensional silicate network structure cannot be formed in such a composition.

Raman spectroscopy is a powerful method for the identification of distinct SiO_4 units in silicate crystals and glasses. The stretching vibration modes of Si–O bonds in silicate crystals and glasses can easily be observed by Raman spectroscopy in the frequency region 800–1200 cm⁻¹. Many earlier investigations of silicate glasses have been reported [6–11]; Mysen and

his coworkers [7, 8] pointed out the coexistence of anionic SiO_4 species such as SiO_4^{4-} monomer (NBO/Si = 4), $Si_2O_7^{6-}$ dimer (NBO/Si = 3), SiO_3^{2-} chain (NBO/Si = 2), $Si_2O_5^{2-}$ sheet (NBO/Si = 1) and SiO_2^0 three-dimensional network unit (NBO/Si = 0) in alkali and alkaline-earth silicate glasses from their Raman results. Iwamoto et al. [9] and Tsunawaki et al. [10] determined the fractions of bridging oxygen, — O — or O^0 (i.e. oxygen co-ordinated to two Si^{4+}), non-bridging oxygen, O^-, (i.e. oxygen co-ordinated to one Si^{4+}) and free or fully-active oxygen, O^{2-} (i.e. oxygen not co-ordinated to Si^{4+}), in PbO–SiO_2, CaO–SiO_2 and CaO–SiO_2–CaF_2 glasses from the Raman intensities of the Si–O stretching bands. More recently, the Raman spectra of rapid quenched Li_2O–SiO_2 glasses were reported [12].

Thermodynamic studies [13–15] emphasized that there is a strong relationship between thermodynamic properties and structural information such as SiO_4 species, and the three species of oxygen: –O– (or O^0), O^- and O^{2-}. Therefore, if quantitative concentrations of the SiO_4 species and three oxygen species in the silicate glasses and melts are obtained by Raman spectroscopy, the thermodynamical properties (e.g. activity) can be unambiguously predicted as quantitative values.

It is the purpose of this study to reveal by Raman spectroscopy detailed structures of Li_2O–SiO_2 glasses containing large amounts of Li_2O ($41.3 \leqslant Li_2O \leqslant 63$ mol %) which could be prepared by rapid quenching. The Raman results are the basis of discussion of the abundance of the SiO_4 units existing in these glasses. Furthermore, an X-ray diffraction (XRD) study was carried out in order to obtain the atomic and co-ordination number.

---

*Author to whom all correspondence should be addressed.

Glass sample	Li_2O (mol%)		SiO_2 (mol%)		NBO/Si number
	Nominal	Analysed	Nominal	Analysed	
$2Li_2O \cdot SiO_2$	67.0	63.0	33.0	37.0	3.405
$3Li_2O \cdot SiO_2$	60.0	59.6	40.0	40.4	2.951
$Li_2O \cdot SiO_2$	50.0	50.4	50.0	49.6	2.032
$2Li_2O \cdot 3SiO_2$	40.0	41.3	60.0	58.7	1.407

2. Experimental procedure

Li_2O–SiO_2 was prepared by a twin-roller apparatus with a thermal-image furnace, as reported previously [1]. Table I provides a list of nominal compositions for the starting materials and compositions, upon analysis, of the glasses prepared.

Raman spectra were measured with a JASCO model R-800 double-grating spectrophotometer. The excitation source was the 51.45 nm (19435.6 cm^{-1}) line of a NEC GLG-3300 Ar–ion laser with power levels from 300 to 400 mW. Each Raman spectrum obtained was deconvoluted into several Gaussian Raman intensities, I_R, composed of several Gaussian peaks as expressed by the following equation.

$$ I_R = \sum_{i=1} I_i \exp \left\{ - \ln 2 \left[\frac{2(\omega - \omega_i)}{\Delta \omega_i} \right]^2 \right\} \quad (1) $$

where I_i, ω_i and $\Delta \omega_i$ are the intensity, position and halfwidth of the peak i, respectively. The area of this Gaussian peak i to the total area, A_i, that is, the relative intensity, is expressed by

$$ A_i = \frac{\frac{1}{2} \left(\frac{\pi}{\ln 2} \right)^{1/2} I_i \Delta \omega_i}{I_R} \simeq \frac{1.064 I_i \Delta \omega_i}{I_R} \quad (2) $$

Deconvolution of the spectra was carried out for digitized scattering data by microcomputer [16].

XRD measurements were carried out with a Rigaku Denki X-ray diffractometer with a rotating anode generator RAD-Ra, with MoK$_{\bar{\alpha}}$ ($\lambda = 0.07107$ nm) radiation under 50 kV and 120 mA. The X-ray scattering intensities were measured from $2\theta = 6$–$140°$ at 0.5° intervals using step scanning with a fixed time of 200 s. After correction for background, polarization and Compton scattering, the coherent X-ray intensity, $I_{eu}^{coh}(S)$, was scaled, by means of the high-angle-region method and the Krogh-Moe/Norman method, to the theoretical intensities due to the independent atoms. The radial distribution functions, $D(r)$, were obtained from the reduced intensities, $S \cdot i(S)$

$$ S \cdot i(S) = S \left[\frac{I_{eu}^{coh}(S)}{\sum\limits_{i=1}^{m} f_i(S)^2} - 1 \right] \quad (3) $$

$$ D(r) = 4\pi r^2 \rho_0 \sum_{i=1}^{m} \bar{K}_i + \sum_{i=1}^{m} (\bar{K}_i)^2 \frac{2r}{\pi} $$

$$ \times \int_0^{S_{max}} S \cdot i(S) \sin (Sr) \, dS \quad (4) $$

where m is the number of atoms contained in the stoichiometric unit, ρ_0 the mean atomic density, $f_i(S)$ the atomic scattering factor of atom i corrected for anomalous dispersion, $\bar{K}_i$ the effective electron number of atom i and S_{max} the maximum value of S ($= 4\pi \sin \theta / \lambda$). The function, $D(r)/r$, calculated from the obtained X-ray intensities was deconvoluted into Gaussian peaks by the nonlinear least-square procedure for the determination of the distances ($r_{ij} \pm 0.001$ nm) and co-ordination numbers ($N_{i/j} \pm 0.1$ atoms) of the nearest-neighbour atomic pairs i–j in these glasses. The density values used for these glasses were determined by the heavy-solution method [3], using a mixture of bromoform and carbon tetrachloride as the heavy solution. The detailed procedure for the measurement and the calculation method of the X-ray data have been reported elsewhere [17, 18].

3. Results and discussion

Fig. 1 shows the Raman spectra of the Li_2O–SiO_2 glasses prepared by rapid quenching. The bands appearing in these Raman spectra can be grouped conveniently into two frequency regions, 500–750 cm^{-1} and 800–1200 cm^{-1}. As shown in Fig. 1, as the Li_2O content increases, the bands at 500–750 cm^{-1}, which
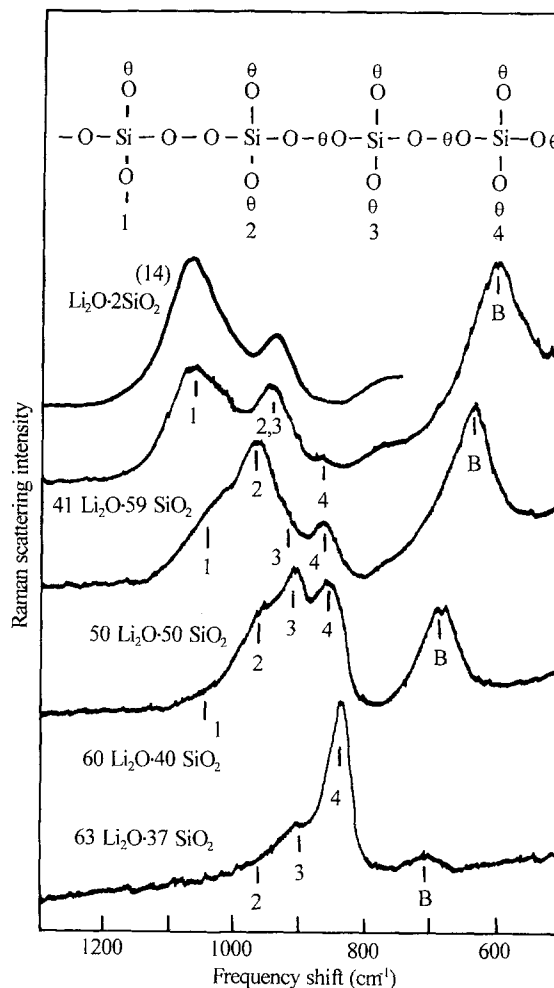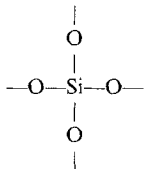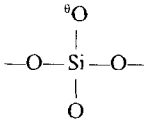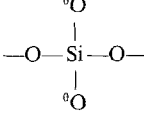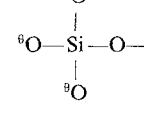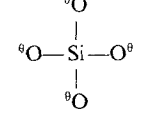

Figure 1 Raman spectra of the rapidly quenched Li_2O–SiO_2 glasses [12]. The Raman spectrum of $Li_2O \cdot 2SiO_2$ ($= Li_2Si_2O_5$) glass [18] is included for comparison.

TABLE II Raman frequencies of the Si–O stretching modes due to SiO_4 units with 0, 1, 3 and 4 NBO/Si in alkali and alkaline-earth glasses [6–11]

SiO_4 unit	Bonding state of bound oxygen	NBO/Si number	Frequency (cm^{-1})
SiO_2^0 three-dimensional network	O | —O—Si—O— | O |	0	1060–1065 1190–1200
$Si_2O_5^{2-}$ sheet	$^\theta$O | —O—Si—O— | O	1	1030–1100
SiO_3^{2-} chain	$^\theta$O | —O—Si—O— | $^\theta$O	2	950–970
$Si_2O_7^{6-}$ dimer	$^\theta$O | $^\theta$O—Si—O— | $^\theta$O	3	850–890
SiO_4^{4-} monomer	$^\theta$O | $^\theta$O—Si—O$^\theta$ | $^\theta$O	4	850–890

Figure 2 Raman spectrum of $63Li_2O \cdot 37SiO_2$ glass deconvoluted into three gaussian peaks due to SiO_3^{2-} chain, $Si_2O_7^{6-}$ dimer and SiO_4^{4-} monomer.

Figure 3 Reduced intensity curves, $S \cdot i(S)$, of $63Li_2O \cdot 37SiO_2$ glass obtained from: (———) XRD, (- - -) a structural model of a SiO_4^{4-} monomer calculated from the Debye scattering equation, and (- · -) Li_4SiO_4 glass derived from MD simulations [4, 5].

are assigned to the bridging Si–O–Si vibration [19] and labelled B, greatly reduced in intensity and shift toward higher frequencies. The continuous intensity drop and shift in the position of the B band with increasing Li_2O content must be related to depolymerization between SiO_4 units. The 800–1200 cm^{-1} frequency region of the measured Raman spectra is attributed to the non-bridging Si–O stretching mode of four SiO_4 units with 1–4 NBO/Si; that is, $Si_2O_5^{2-}$ sheet, SiO_3^{2-} chain, $Si_2O_5^{6-}$ dimer and SiO_4^{4-} monomer [7–11]. As summarized in Table II, these four Raman modes caused by the SiO_4 units with 1–4 NBO/Si appear at 1030–1100 cm^{-1}, 950–970 cm^{-1}, 900–930 cm^{-1}, and 850–890 cm^{-1}, respectively. In glasses containing a relatively small amount of Li_2O, the main peaks are the bands due to the $Si_2O_5^{2-}$ sheet and SiO_3^{2-} chain. In glasses containing a large amount of Li_2O, however, bands due to $Si_2O_5^{6-}$ dimer and SiO_4^{4-} monomer are mainly observed. These Raman results indicate that the SiO_4 units with higher NBO/Si ratios increase with increasing Li_2O content because of the depolymerization of SiO_4 units.

Fig. 2 shows the Raman spectrum of $63Li_2O \cdot 37SiO_2$ glass deconvoluted into three Gaussian peaks due to a SiO_4^{4-} monomer, a $Si_2O_5^{6-}$ dimer and a SiO_3^{2-} chain. As can be seen, most of the SiO_4 tetrahedra in the glass with the highest Li_2O content are present as isolated SiO_4 units such as SiO_4^{4-} monomer and $Si_2O_5^{6-}$ dimer. This fact was also recognized from the X-ray analysis and MD simulation
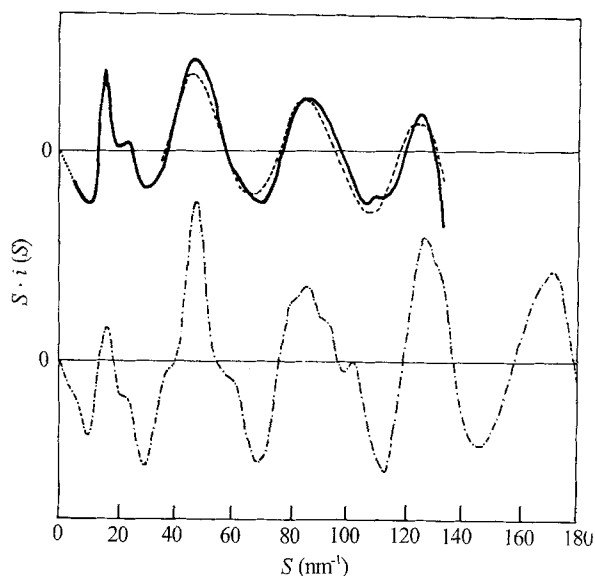
results [4, 5] for this glass. Using the Debye scattering equation [20] given by

$$S \cdot i(S) \left[\sum_{i=1}^{m} f_i(S)^2 \right] = \sum_{i=1}^{m} \sum_{j=1}^{m} {}_{(i \neq j)} N_{i/j} f_i(S) f_j(S)$$
$$\times \exp(-b_{i-j}S^2) \frac{\sin(Sr_{i-j})}{r_{i-j}} \quad (5)$$

where r_{i-j} and $N_{i/j}$ are the distance and co-ordination number of the nearest-neighbour ionic i–j pair, respectively, and b_{i-j} is the temperature factor, i.e. half the mean-square variation in r_{i-j}. The reduced intensity, $S \cdot i(S)$, was calculated for a structural model of a SiO_4^{4-} monomer, in which four lithium ions occupy four corner sites in order to satisfy the stoichiometric unit of Li_4SiO_4 composition. Excellent agreement for three $S \cdot i(S)$ curves can be seen in Fig. 3.

TABLE III Relative intensity of the Gaussian peaks of four SiO_4 units with 1-4 NBO/Si, and fractions of O^0, O^- and O^{2-} in the rapidly quenched Li_2O-SiO_2 glasses

Glass sample (mol %)	Relative intensity[a] (%)				Oxygen fraction (%)		
	$Si_2O_5^{2-}$ sheet	SiO_3^{2-} chain	$Si_2O_7^{6-}$ dimer	SiO_4^{4-} monomer	O^0	O^-	O^{2-}
$63Li_2O \cdot 37SiO_2$	0	9.3	34.3	56.5	4.3	82.2	13.5
	0[b]	3.1[b]	28.1[b]	37.2[b]	5[b]	90[b]	5[b]
$60Li_2O \cdot 40SiO_2$	5.2	30.5	35.4	28.9	16.0	82.3	1.7
$50Li_2O \cdot 50SiO_2$	15.5	60.6	9.4	12.4	29.7	70.3	–
$41Li_2O \cdot 59SiO_2$	65.6	33.0	–	6.3	48.9	51.1	–

[a] Peak area to total-area represented by Equation 1
[b] MD results [4, 5] of Li_4SiO_4 glass at 300 K.

The relative intensity of each Raman band in the frequency range 800–1200 cm^{-1} is associated with the abundance of SiO_4 units giving rise to the stretching vibration of the Raman bands listed in Fig. 1. Before determining the proportions of the SiO_4 units with 1–4 NBO/Si in the rapidly quenched Li_2O-SiO_2 glasses, the normalized Raman cross-sections of the four SiO_4 units with 1–4 NBO/Si empirically checked by means of the method proposed by Mysen et al. [21, 22]. The relative intensity, A_i, of Raman-band i is related to the proportion (mole fraction) of SiO_4-unit i, x_i, by the following equation:

$$x_i = \alpha_i A_i \qquad (6)$$

where α_i is the normalized Raman cross-section of SiO_4-unit i, and A_i in Equation 6 corresponds to the ratio of the area of Gaussian peak i to the total area represented by Equation 2, that is, the relative intensity. Table III lists the values of the relative intensities of these Raman bands due to the four SiO_4 units with 1–4 NBO/Si. The α_i are then related to A_i, and are

mass balanced with the number of NBO/Si, n_i, which is 1, 2, 3 and 4 for $Si_2O_5^{2-}$ sheet, SiO_3^{2-} chain, $Si_2O_7^{6-}$ dimer and SiO_4^{4-} monomer, respectively. Consequently, the summation of n_i is equal to the bulk NBO/Si [21, 22], which can be calculated from the analysis in Table I as follows

$$\sum \alpha_i A_i n_i = NBO/Si \qquad (7)$$

$$\sum \alpha_i A_i = 1 \qquad (8)$$

In the rapidly quenched Li_2O-SiO_2 glasses, the α_i factors calculated from Equations 6–8 were 1.04, 1.02, 1.15 and 0.90 for $Si_2O_5^{2-}$ sheet, SiO_3^{2-} chain, $Si_2O_7^{6-}$ dimer and SiO_4^{4-} monomer, respectively. These estimated α_i factors indicate that the scattering efficiencies of the four SiO_4 units with 1, 2, 3 and 4 NBO/Si are almost equivalent. Therefore, the relative intensity of the Raman bands listed in Table III directly corresponds to the proportions of these four SiO_4 units present in the rapidly quenched Li_2O-SiO_2 glasses.

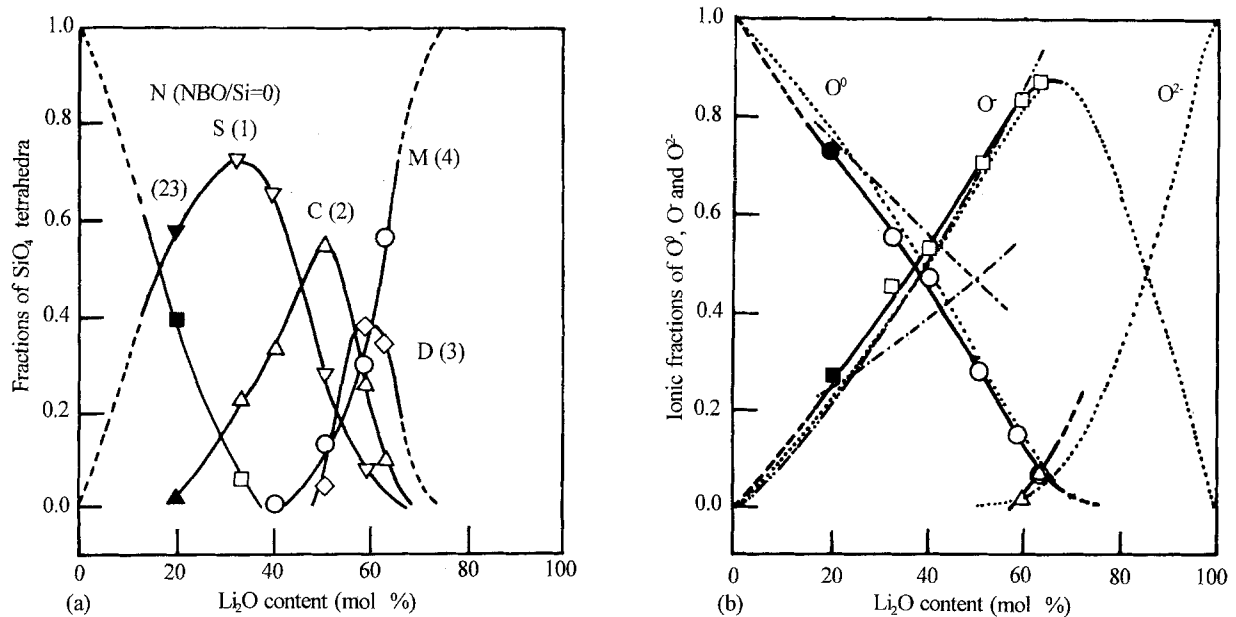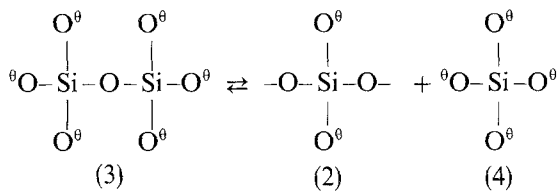Fig. 4 shows the proportions of SiO_4 units with 0–4

Figure 4 Proportions of: (a) SiO_4 units with 0, 1, 2, 3 and 4 NBO/Si, and (b) fractions of O^0, O^- and O^{2-} in the rapidly quenched Li_2O-SiO_2 glasses. The Raman data $Rb_2O \cdot 4SiO_2$ (= $Rb_2Si_4O_9$) glass [23] are included for comparison: (—·—) the proportions of O^0, O^- and O^{2-} obtained from X-ray-photoelectron-spectroscopy measurements [24], (· · ·) the proportion of O^0, O^- and O^{2-} calculated from Yokokawa and Niwa's thermodynamic model [26, 28] by using an optimal equation constant, K(= 0.0078), derived from the Raman analyses, (- · · -) the proportion of O^- can be given by $2x/(1-x)$ if the compositional formula of the rapidly quenched Li_2O-SiO_2 glasses is regarded as $xLi_2O \cdot (1-X)SiO_2$.

NBO/Si and the fractions of bridging oxygen –O– or O^0 (i.e. oxygen co-ordinated to two Si^{4+}), non-bridging oxygen, O^- (i.e. co-ordinated to one Si^{4+}), and free or fully-active oxygen, O^{2-} (i.e. not co-ordinated to Si^{4+}) in the rapidly quenched Li_2O–SiO_2 glasses as a function of the Li_2O content. Fig. 4 also contains the previously obtained data [23] for $Li_2O \cdot 2SiO_2$ ($= Li_2Si_2O_5$) described above. The content of $Si_2O_7^{6-}$ dimer (NBO/Si = 3), SiO_3^{2-} chain (NBO/Si = 2) and $Si_2O_5^{2-}$ sheet (NBO/Si = 1) have a maximum at approximately 60, 50 and 33 mol % Li_2O, respectively. These Li_2O contents correspond to $Li_6Si_2O_7$ (NBO/Si = 3), Li_2SiO_3 (NBO/Si = 2) and $Li_2Si_2O_5$ (NBO/Si = 1), respectively. The proportion of SiO_2^0 three-dimensional network units (NBO/Si = 0) remarkably decreases with increasing Li_2O content. This result of the Raman analysis, illustrated in Fig. 4, suggests that no glass is composed of only one SiO_4 unit. For example, the fact that the $63Li_2O \cdot 37SiO_2$ glass consists not only of SiO_4^{4-} monomer but also of $Si_2O_7^{6-}$ dimer and SiO_3^{2-} chain suggests that the glass structure should arise from the following equilibrium reaction

$$
\begin{array}{cccc}
O^\theta & O^\theta & O^\theta & O^\theta \\
| & | & | & | \\
{}^\theta O{-}Si{-}O{-}Si{-}O^\theta \rightleftarrows & {-}O{-}Si{-}O{-} & + & {}^\theta O{-}Si{-}O^\theta \\
| & | & | & | \\
O^\theta & O^\theta & O^\theta & O^\theta \\
(3) & & (2) & (4)
\end{array}
$$

This analysis of the Raman results shows a satisfactory agreement with ^{29}Si magic-angle spinning (MAS) NMR results [25] in the Li_2O–SiO_2 glasses ($15 \leqslant Li_2O \leqslant 40$ mol %) prepared by the usual melt–cooling method, as shown in Fig. 5. This Raman result is also in quantitatively satisfactory agreement with MD simulation results [4, 5], as indicated in Table III. More recently, Dorfeld [15] estimated the concentration of SiO_4 units in Na_2O–SiO_2 glasses at
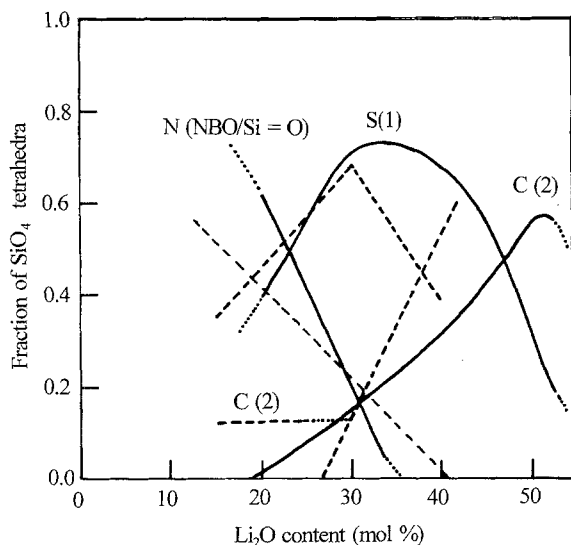
300 K as a function of glass composition from an ideal chemical model. Dorfeld's values are in reasonable agreement with those derived from our Raman results.

As previously mentioned, oxygen ions in the silicate glasses can be generally classified as bridging oxygen, O^0, non-bridging oxygen, O^-, or free or fully-active oxygen, O^{2-}. As indicated in Table III the fractions of O^0, O^- and O^{2-} in the $63Li_2O \cdot 37SiO_2$ glass derived from the Raman results were 4, 83 and 13%, respectively. However, the proportions of O^0, O^- and O^{2-} calculated from MD simulations [4, 5] were 5, 90 and 5%, respectively. The agreement with these Raman and MD [4, 5] values is satisfactory. Furthermore, as shown in Fig. 4b, comparison of the fractions of O^0, O^- and O^{2-} obtained from the Raman results with those calculated on the basis of a thermodynamic model proposed by Yokokawa and Niwa [26] gives an excellent agreement. In Fig. 6, the ratios of bridging to non-bridging oxygen, R ($= N_{O^0}/N_{O^-}$), are compared with the values predicted for each glass from its composition and charge-balance considerations and the modified random network (MRN) model [27]. All ratios are found to agree with the predicted values. The equilibrium constant, K, of the reaction $2O^- \rightleftarrows O^0 + O^{2-}$ between O^0, O^- and O^{2-} can be given by the following equation [13, 14]

$$ K = \frac{[O^0][O^{2-}]}{[O^-]^2} \tag{9} $$

The Raman-estimated value K calculated from Equation 9 is 0.0078, which is in reasonable agreement with the value of 0.0032 for the Li_4SiO_4 glass at 300 K obtained from MD simulations [4, 5]. Yokokawa and Niwa [26] estimated the K values to be 0.14–0.003 for $M^{2+}O$–SiO_2 binary melts (where M is either Mn, Pb or Ca) from a thermodynamic calculation. It is presumed that the value K relates to the cohesive energy of the network-modifying oxides, Ma_2O (where Ma is
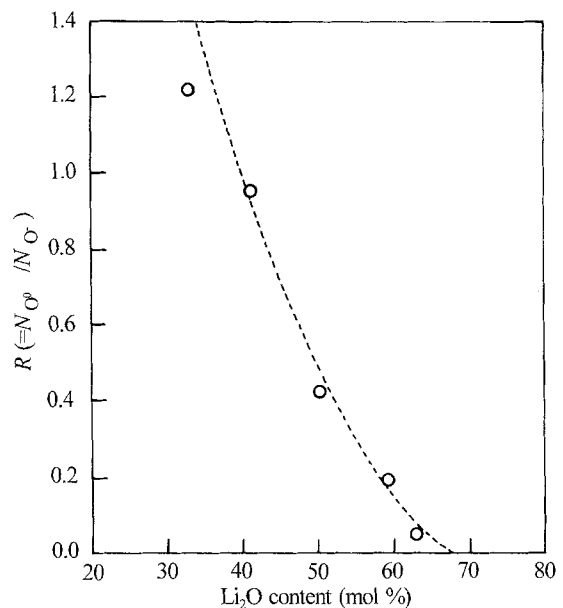

Figure 5 Comparison of the proportions of SiO_4 units in the Li_2O–SiO_2 glasses determined by: (———) our Raman and (– – –) Shramm and de Jong's ^{29}Si MAS NMR [25] analyses. Included in this figure for comparison are the Raman results for $Rb_2O \cdot 4SiO_2$ ($= Rb_2Si_4O_9$) glass [23].

Figure 6 Ratio of bridging to non-bridging oxygen, R ($= N_{O^0}/N_{O^-}$): (○) rapidly quenched Li_2O–SiO_2 glasses derived from the Raman results showing agreement with (– – –) the values predicted from the glass composition.

an alkali metal), such as Li_2O in silicate melts and glass [26]. Usually a lowering bond strength, $z_{Ma}/(r_{Ma^+} + r_{O^{2-}})$ (where z_{Ma} is the formal charge of the Ma^+ ion, r_{Ma^+} and $r_{O^{2-}}$ are the ionic radii of ions Ma^+ and O^{2-}), between Ma^+ and O^{2-} tends to decrease the value of K [26]. It is, therefore, concluded that the value of K for the $63Li_2O \cdot 37SiO_2$ glass is much smaller than that for the $CaO-SiO_2$ [26]. From the value obtained for K, it is possible to predict that the activity coefficient is one of the most important thermodynamic parameters. Therefore, by the use of the following Yokokawa and Niwa equations [26, 28]

$$a_{SiO_2} = \left\{ \frac{2x_{SiO_2}}{1 + x_{SiO_2}} - 1 - \left[\frac{8x_{SiO_2}x_{Li_2O}(1 - 4K)}{2(1 - 4K)} \right]^{1/2} \right\}^2$$
$$\left(\frac{1 + x_{SiO_2}}{2x_{SiO_2}} \right)^3 \tag{10}$$

and

$$a_{Li_2O} = \left\{ \frac{x_{Li_2O}}{1 + x_{SiO_2}} - \frac{1 - \left[\frac{1 - 8x_{SiO_2}x_{Li_2O}(1 - 4K)}{(1 + x_{Li_2O})^2} \right]^{1/2}}{2(1 - 4K)} \right\}^{3/2} \left(\frac{1 + x_{SiO_2}}{x_{Li_2O}} \right)^{3/2} \tag{11}$$

and the value obtained for K the activity curves of Li_2O and SiO_2 for the Li_2O-SiO_2 glasses at 300 K were calculated, as indicated in Fig. 7.

By using the proportions of the four SiO_4 units present in the rapidly quenched Li_2O-SiO_2 glasses, the average co-ordination numbers were determined for the nearest-neighbour atomic pairs Si–Si, O–Si and O–O; i.e. $N_{Si/Si}$, $N_{O/Si}$ and $N_{O/O}$ were determined. These co-ordination numbers can be estimated using the following two methods.

Method 1. Table IV shows the average co-ordination numbers of the nearest-neighbour correlations Si–Si, O–Si and O–O for the SiO_4 units with 0, 1, 2, 3 and 4 NBO/Si, i.e. $n_{Si/Si}$, $n_{O/Si}$ and $n_{O/O}$. The relationship between the bulk- and SiO_4-unit's co-ordination

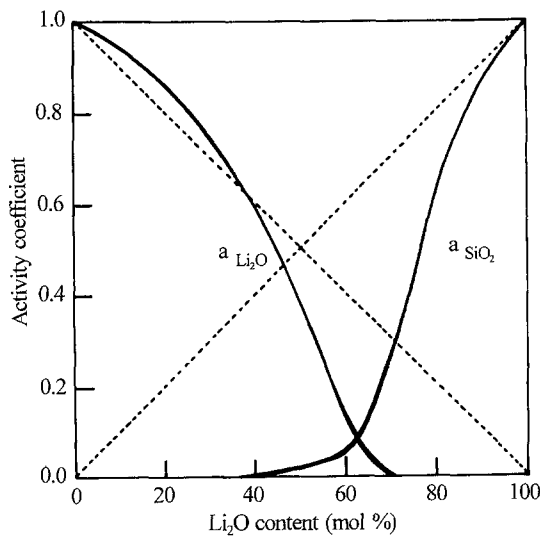*Figure 7* Activity curves for binary Li_2O-SiO_2 glass at 300 K calculated from Yokokawa and Niwa's model [26, 29] by using an optimal equilibrium constant K (= 0·0078) derived from Raman analysis.
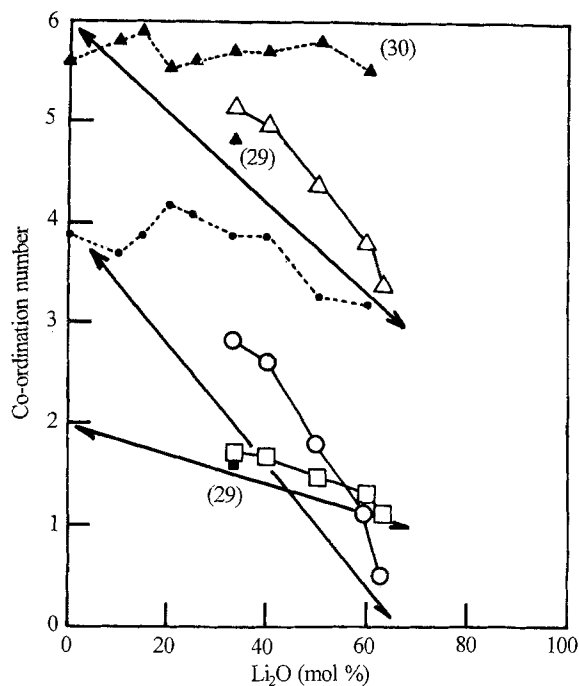
numbers can be given as follows

$$N_{Si/Si} = 3f_{(NBO/Si = 1)} + 2f_{(2)} + 3f_{(3)} \tag{12}$$

$$N_{O/Si} = 1.75f_{(1)} + 1.50f_{(2)} + f_{(4)} \tag{13}$$

$$N_{O/O} = 5.25f_{(1)} + 4.50f_{(2)} + 3f_{(4)} \tag{14}$$

where $f_{(i)}$ ($i = 1-4$) is the proportion of the SiO_4 unit with NBO/Si = i as indicated in Table III.

Method 2. The fractions of O^0, O^- and O^{2-} can be given by the following equations

$$N_{Si/Si} = 4N_{O^0} \tag{15}$$

$$N_{O/Si} = 2N_{O^0} + N_{O^-} \tag{16}$$

$$N_{O/O} = 6N_{O^0} + 3N_{O^-} \tag{17}$$

where N_{O^0}, N_{O^-} and $N_{O^{2-}}$ are the fractions of O^0, O^- and O^{2-} as listed in Table III.

The results calculated from methods 1 and 2 are shown graphically in Figs 8 and 9, respectively, the values $N_{Si/Si}$, $N_{O/Si}$ and $N_{O/O}$ estimated from these two methods drop reasonably with the increase in Li_2O content due to a depolymerization reaction between SiO_4 units. This tendency of these co-ordination numbers confirms the prediction from simple considera-

TABLE IV Co-ordination numbers of nearest-neighbour correlations Si–Si, O–Si and O–O for SiO_4 units with 0, 1, 2, 3 and 4 NBO/Si

SiO_4 unit	Bonding state of bound oxygen	NBO/Si number	Co-ordination number		
			$n_{Si/Si}$	$n_{O/Si}$	$n_{O/O}$
SiO_2^0 three-dimensional network	O | —O—Si—O— | O	0	4.00	2.00	6.00
$Si_2O_5^{2-}$ sheet	$^\theta$O | —O—Si—O— | O	1	3.00	1.75	5.25
SiO_3^{2-} chain	$^\theta$O | —O—Si—O— | $^\theta$O	2	2.00	1.50	4.50
$Si_2O_7^{6-}$ dimer	$^\theta$O | $^\theta$O—Si—O— | $^\theta$O	3	1.00	1.25	3.75
SiO_4^{4-} monomer	$^\theta$O | $^\theta$O—Si—O$^\theta$ | $^\theta$O	4	0	1.00	3.00

Figure 8 Composition dependence of co-ordination numbers of nearest-neighbour pairs Si–Si, O–Si and O–O in the rapidly quenched Li_2O–SiO_2 glasses obtained from Raman analysis by means of Method 1: (——) co-ordination numbers estimated from composition dependence of silicate glass structure, ($\bigcirc$, $\bullet$) $N_{Si/Si}$, ($\square$, $\blacksquare$) $N_{O/Si}$, ($\triangle$, $\blacktriangle$) $N_{O/O}$. The data for $Li_2O \cdot 2SiO_2$ glass obtained from neutron diffraction measurement by Hannon *et al.* [29] and for Na_2O–SiO_2 melts obtained from XRD measurement [30] are included for comparison.
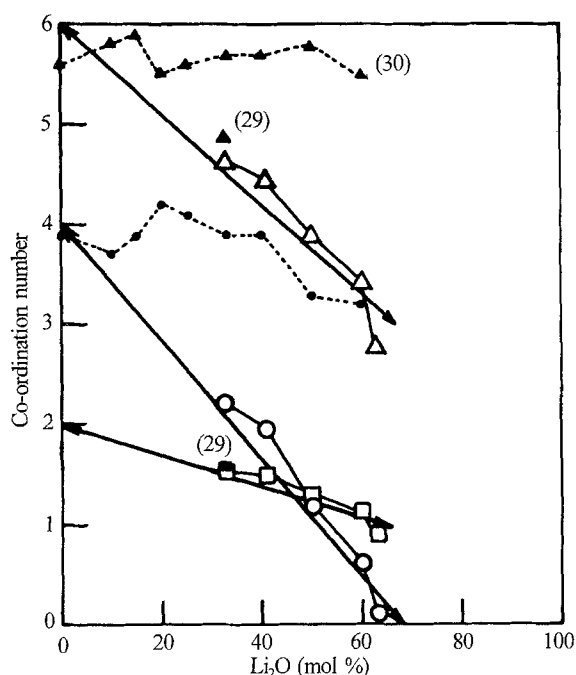

Figure 9 Composition dependence of co-ordination numbers of nearest-neighbour pairs Si–Si, O–Si and O–O in the rapidly quenched Li_2O–SiO_2 glasses obtained from Raman analysis by means of Method 2: (——) co-ordination numbers estimated from composition dependence of silicate glass structure, ($\bigcirc$, $\bullet$) $N_{Si/Si}$, ($\square$, $\blacksquare$) $N_{O/Si}$, ($\triangle$, $\blacktriangle$) $N_{O/O}$. Data for $Li_2O \cdot 2SiO_2$ glass obtained from neutron diffraction measurement by Hannon *et al.* [29] and for Na_2O–SiO_2 melts obtained from XRD measurement [30] are included for comparison.

tion on the basis of composition dependence and charge balance of alkali-silicate-glass structure. For instance, the $N_{O/O}$ value of the $63Li_2O \cdot 37SiO_2$ glass is $2.7 \sim 3.4$, and is almost equal to the values obtained from XRD ($N_{O/O} = 3.3$) and MD simulations [4, 5] ($N_{O/O} = 3.3$). More recently, Hannon *et al.* [29] have studied the structure of three alkali silicate glasses of nominal composition $M_2O \cdot 2SiO_2$ (with $M = K$, $K_{0.46}Li_{0.54}$ and Li) with a high-resolution neutron diffractometer. The values for $N_{O/Si}$ and $N_{O/O}$ of the $Li_2O \cdot SiO_2$ glass reported from the neutron results [29] are 1.61 and 4.81, respectively; these values are also equal to the values estimated from the two methods outlined above, as shown in Figs 8 and 9. Values of the co-ordination numbers for molten Na_2O–SiO_2, obtained from XRD measurements by Waseda *et al.* [30] are included for comparison. Waseda and his coworkers systematically carried out X-ray structural analyses of alkali and alkaline-earth silicate melts [31]. As shown in Figs 8 and 9, Waseda's results, unfortunately, indicate that the addition of Na_2O up to 60 mol% has no effect on $N_{Si/Si}$ and $N_{O/O}$ in the molten Na_2O–SiO_2 system [30], which is not in agreement with our Raman results. When Ma_2O (where Ma is an alkali metal) is added to an SiO_2 melt and/or glass, it is widely accepted that physical properties such as viscosity drastically change [33], owing to the rupture of three-dimensional network structure. In the MRN model [27], the addition of one network modifier unit, Ma_2O, causes one bridging oxygen (BO) between two connected tetrahedra to be replaced by two non-bridging oxygen (NBO) atoms. The negative charge on the singly charged NBOs is balanced by the positively charged Ma^+ ions. Therefore, the authors consider that there is room for the X-ray results reported by Waseda and his coworkers [30–32] to be remeasured.

The $S \cdot i(S)$ curves for the rapidly quenched Li_2O–SiO_2 glasses are shown in Fig. 10. Periodical profiles of the curves are very similar to each other among these glasses with different composition. The increase in the Li_2O content, however, causes the change of the peak in the S region below about $30\ nm^{-1}$. This feature of the $S \cdot i(S)$ curves may correspond to a change in the atomic configuration of the mid- and long-range region of SiO_4 units caused by depolymerization with increasing Li_2O content. The average atomic distances and co-ordination numbers for nearest-neighbour pairs Si–O, Li–O, O–O and Si–Si derived from the function $D(r)/r$ of Fig. 11 are listed in Table V. The data for Li_4SiO_4, $Li_6Si_2O_7$, Li_2SiO_3 and $Li_2Si_2O_5$ crystals [35–38] are included for comparison. From this table, the average bond length of an Si–O pair, $r_{Si–O}$, tends to increase from 0.160 to 0.164 nm with the increase in Li_2O content, this is due to the weakening of the Si–O bond, due to the introduction of a modifier oxide into the silicate-network structure [39]. Misawa *et al.* [34] reported a similar elongation of the Si–O bond length in three alkali disilicate glasses from a time-of-flight total neutron scattering experiment. Although the co-ordination number of nearest-neighbour oxygen around silicon, $N_{Si/O}$, is almost equal to 4 because

TABLE V Atomic distances and co-ordination numbers of nearest-neighbour pairs Si–O, Li–O, O–O and Si–Si in the rapidly quenched Li_2O–SiO_2 glasses determined from X-ray analysis. Data for lithium disilicate glass [29, 31, 34] and several Li_2O–SiO_2 crystals [35–38] are included for comparison.

Glass sample (mol %)	Atomic distance (nm)				Co-ordination number	
	$r_{Si–O}$	$r_{Li–O}$	$r_{O–O}$	$r_{Si–Si}$	$N_{Si/O}$	$N_{Li/O}$
$63Li_2O \cdot 37SiO_2$	0.164	0.223	0.272	0.320	4.0	3.1
	0.160^a	0.193^a	0.259^a	0.310^a	4.0^a	$3–4^a$
$60Li_2O \cdot 40SiO_2$	0.163	0.221	0.268	0.315	3.8	2.4
$50Li_2O \cdot 50SiO_2$	0.161	0.221	0.264	0.314	4.3	2.2
$41Li_2O \cdot 59SiO_2$	0.161	0.224	0.274	0.20	4.5	2.0
$Li_2O \cdot 2SiO_2^b$	0.1630	0.1968	0.2660		3.80	2.16
$Li_2O \cdot 2SiO_2^c$	0.162	0.207	0.265	0.313	3.7	3.8
$Li_2O \cdot 2SiO_2^d$	0.1624		0.265		3.9	
Li_4SiO_4 crystal^e	0.163	0.211			4	4–6
$Li_6Si_2O_7$ crystal^d	0.164	0.207			4	4–5
Li_2SiO_3 crystal^d	0.163	0.207			4	4
$Li_2Si_2O_5$ crystal^d	0.163	0.195			4	4

^{a} MD results [4, 5] of Li_4SiO_4 glass at 300 K.
^{b} [29]; ^{c} [31]; ^{d} [34]; ^{e} [35–38].
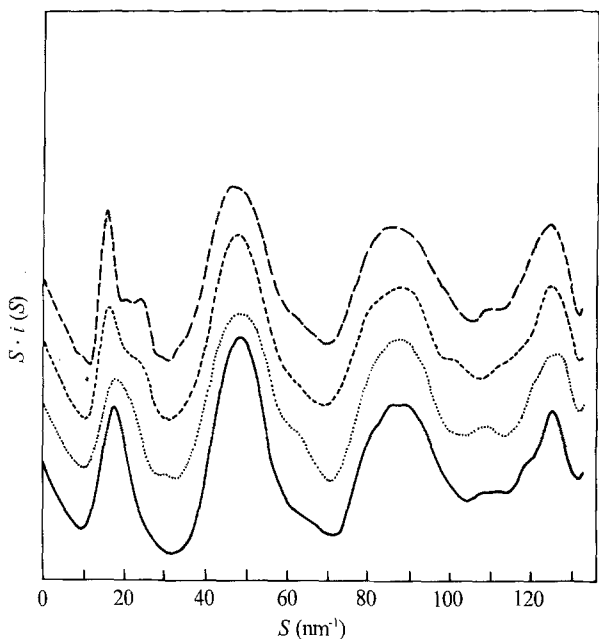
Figure 10 X-ray reduced intensity curves $S \cdot i(S)$ for the rapidly quenched Li_2O–SiO_2 glasses: (– – –) $63Li_2O \cdot 37SiO_2$, (- - -) $60Li_2O \cdot 40SiO_2$, (· · ·) $50Li_2O \cdot 50SiO_2$, and (———) $41Li_2O \cdot 59SiO_2$.
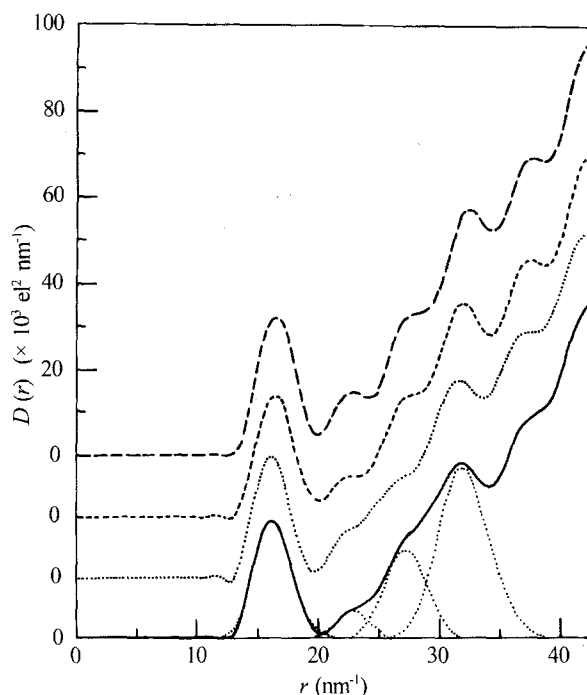
Figure 11 Radial distribution function curves $D(r)$ for the rapidly quenched Li_2O–SiO_2 glasses: (– – –) $63Li_2O \cdot 37SiO_2$, (- - -) $60Li_2O \cdot 40SiO_2$, (. . .) $50Li_2O \cdot 50SiO_2$, and (———) $41Li_2O \cdot 59SiO_2$.

of SiO_4 tetrahedra, the co-ordination number around lithium, $N_{Li/O}$, is increased from 2.0 for $41Li_2O \cdot 59SiO_2$ glass to 3.1 for $63Li_2O \cdot 37SiO_2$ glass with increasing Li_2O content. As shown in Table V, in the lithium-silicate crystal structures [35–38] lithium ions are co-ordinated with 4–6 oxygen ions, whereas the $N_{Li/O}$ values for the rapidly quenched Li_2O–SiO_2 glasses obtained from the X-ray results are much smaller than those of crystals [34–37]. The small $N_{Li/O}$ values are in accordance with the results of MD results [4, 5] for the Li_4SiO_4 glass. Furthermore, the present result is also supported by the results of Hannon et al. [29] who have shown (in a high-resolution-

neutron-diffraction study of three alkali silicate glasses of nominal composition $M_2O \cdot 2SiO_2$ where M is K, $K_{0.46}Li_{0.54}$ or Li) that $N_{Li/O}$ is 2.16 for the $Li_2O \cdot 2SiO_2$ glass. According to Hannon et al. [29], if a lithium ion has only NBO in its first oxygen co-ordination shell then the number of lithium ions which are first neighbours to a NBO is $N_{O/Li}/f_{NBO}$, which is calculated to be 2.18, suggesting a simple pairing of lithiums between two non-bridging oxygens, thus

$$\begin{array}{ccc} | & Li^+ & | \\ —Si—O^- & & {}^-O—Si— \\ | & Li^+ & | \end{array}$$
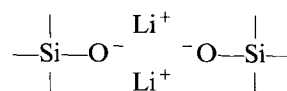
4. Conclusion

The results of Raman analysis of the rapidly quenched Li_2O-SiO_2 glasses lead to the conclusion that the Raman relative intensities of the four SiO_4 units with 1, 2, 3 and 4 NBO/Si in these glasses are equivalent to the abundances of the corresponding SiO_4 units. By the use of the proportions of the SiO_4 units and the fractions of bridging, non-bridging and free or fully active oxygen, the co-ordination numbers were determined for the nearest-neighbour pairs, Si-Si, O-Si and O-O in Li_2O-SiO_2 glasses. As a result, the co-ordination numbers obtained reasonably drop with the increase in the Li_2O content due to the depolymerization reaction between SiO_4 units. Furthermore, in order to obtain structural information on the Li_2O-SiO_2 glasses, XRD measurements were carried out. The X-ray results showed an increase in the average atomic distance of the Si-O pair with increasing Li_2O content due to the weakening of the Si-O bond. Lithium ions are found to be coordinated by $2 \sim 3$ oxygen ions.

References

1. M. TATSUMISAGO, T. MINAMI and M. TANAKA, *J. Am. Ceram. Soc.* **64** (1981) C-97.
2. *Idem J. Ceram. Soc. Jpn.* **93** (1985) 581.
3. M. TATSUMISAGO, M. TAKAHASHI and T. MINAMI, *Chem. Express* **1** (1986) 91.
4. N. IWAMOTO, N. UMESAKI, M. TAKAHASHI, M. TATSUMISAGO. T. MINAMI and Y. MATSUI, *J. Non-Cryst. Solids* **95/96** (1987) 233.
5. N. UMESAKI, N. IWAMOTO, M. TAKAHASHI, M. TATSUMISAGO, M. MINAMI and Y. MATSUI, *Trans. Iron Steel Inst. Jpn.* **28** (1988) 852.
6. S. A. BRAWER and W. B. WHITE. *J. Chem. Phys.* **63** (1975) 2421.
7. B. O. MYSEN, D. VIRGO and C. M. SCARE, *Am. Mineral.* **65** (1980) 690.
8. D. VIRGO, B. O. MYSEN and T. KUSHIRO, *Science* **208** (1980) 1371.
9. N. IWAMOTO, Y. TSUNAWAKI and S. MIYAGO, *Trans. Jpn. Inst. Metals* **43** (1979) 1138.
10. T. TSUNAWAKI, N. IWAMOTO, T. HATTORI and A. MITSUISHI, *J. Non-Cryst. Solids* **44** (1981) 369.
11. T. FURUKAWA, K. E. FOX and W. B. WHITE, *J. Chem. Phys.* **75** (1980) 3226.
12. M. TATSUMISAGO, M. TAKAHASHI, T. MINAMI, N. UMESAKI and N. IWAMOTO, *Chem. Lett.* (1986) 1371.
13. C. J. B. FINCHAM and F. D. RICHARDSON, *Proc. R. Soc.* **A 223** (1954) 40.
14. G. W. TOOP and C. S. SAMIS, *Trans. Metall. Soc. A.I.M.E.* **224** (1962) 878.
15. W. G. DORFELD, *Phys. Chem. Glasses* **29** (1988) 179.
16. M. TATSUMISAGO, M. TAKAHASHI, T. MINAMI, M. TANAKA, N. UMESAKI, and N. IWAMOTO, *J. Ceram. Soc. Jpn.* **94** (1986) 464.
17. N. IWAMOTO, N. UMESAKI, S. GOTO, T. HANADA and N. SOGA, *J. Non-Cryst. Solids* **70** (1985) 1775.
18. N. IWAMOTO, N. UMESAKI and K. DOHI, *J. Jpn. Inst. Metals* **47** (1983) 382.
19. R. J. BELL and P. DEANS, *Dicuss. Faraday Soc.* **50** (1970) 55.
20. N. UMESAKI, N. IWAMOTO, H. OHNO and K. FURUKAWA, *J. Chem. Soc. Faraday Trans. I* **78** (1982) 382.
21. B. O. MYSEN, L. W. FINGER, D. VIRGO and F. A. SEIFERT, *Am. Mineral.* **67** (1982) 686.
22. B. O. MYSEN, D. VIRGO and F. A. SEIFERT, *Am. Mineral.* **70** (1985) 88.
23. N. IWAMOTO, N. UMESAKI and K. DOHI, *J. Jpn Ceram. Soc.* **92** (1984) 201.
24. H. SUGINOHARA, *Bull. Jpn Inst. Metals* **19** (1980) 30.
25. C. M. SCHRAMM, B. H. W. S. de JONG and V. E. PARZIALE, *J. Am. Chem. Soc.* **106** (1984) 4396.
26. T. YOKOKAWA and K. NIWA, *Trans. JIM* **10** (1969a) 3.
27. B. E. WARREN and J. BISCOE, *J. Am. Ceram. Soc.* **21** (1938) 259.
28. K. NAKAMURA, "Materials science of the earth, in the Iwatani earth science series, Vol. 3, II" edited by S. Akimoto and H. Mizutani (Iwatani Shoten, 1982) p. 206–225.
29. A. C. HANNON, B. VESSAL and J. M. PARKER, The Fifth International Conference on the Structure of Non-Crystalline Materials (NCM5), Sendai, Japan, September 1991, *J. Non-Cryst. Solids* **150** (1992) 97.
30. Y. WASEDA and H. SUITO, *Iron Steel Inst. Jpn.* **17** (1977) 82.
31. Y. WASEDA, *Prog. Mater. Sci.* **26** (1981) p. 81–106.
32. Y. WASEDA and J. M. TOGURI, *Met. Trans.* **B8** (1977) 563.
33. H. SCHOLZE, in "Glass: nature, structure, and properties", (Springer-Verlag, 1990) p. 156–181.
34. M. MISAWA, D. L. PRICE and K. SUZUKI, *J. Non-Cryst. Solids* **37** (1980) 85.
35. H. VOLLENKLE, A. WITTMANN and H. NOWOTNY, *Mh. Chem.* **99** (1968) 1360.
36. *Idem, ibid.* **100** (1969) 295.
37. F. LIEBAU, *Acta Cryst.* **14** (1961) 251.
38. H. SEEMAN, *ibid.* **9** (1956) 251.